HHS Public Access

Author manuscript

Bioorg Med Chem Lett. Author manuscript; available in PMC 2023 July 15.

Published in final edited form as:

Bioorg Med Chem Lett. 2022 July 15; 68: 128718. doi:10.1016/j.bmcl.2022.128718.

Quinazolinones as allosteric fourth-generation EGFR inhibitors for the treatment of NSCLC

Thomas W. Gero[a,b], **David E. Heppner**[a,b,1], **Tyler S. Beyett**[a,b], **Ciric To**[c,d,e], **Seth C. Azevedo**[a,b], **Jaebong Jang**[a,b], **Thomas Bunnell**[a,b], **Frederic Feru**[a,b], **Zhengnian Li**[a,b], **Bo Hee Shin**[c,d,e], **Kara M. Soroko**[f], **Prafulla C. Gokhale**[f], **Nathanael S. Gray**[a,b,2], **Pasi A. Jänne**[c,d,e], **Michael J. Eck**[a,b], **David A. Scott**[a,b]

[a]Department of Cancer Biology, Dana-Farber Cancer Institute, Boston, MA 02115, USA.

[b]Department of Biological Chemistry & Molecular Pharmacology, Harvard Medical School, 360 Longwood Ave, Boston, MA 02115, USA.

[c]Lowe Center for Thoracic Oncology, Dana-Farber Cancer Institute, Boston, MA 02215, USA.

[d]Department of Medical Oncology, Dana-Farber Cancer Institute, Boston, MA 02215, USA.

[e]Department of Medicine, Harvard Medical School, Boston, MA 02115, USA.

[f]Experimental Therapeutics Core and Belfer Center for Applied Cancer Science, Dana-Farber Cancer Institute, Boston MA 02215, USA.

Graphical Abstract

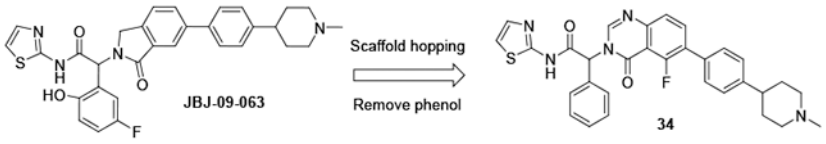

More than 60 kinase inhibitors have been approved by the FDA, with new approvals each year for oncology and other indications.[1, 2] The epidermal growth factor receptor (EGFR) is one of the most intensively studied kinases, with three generations of targeted therapeutic drugs for the treatment of lung cancer.[3] Non small-cell lung cancer (NSCLC) patients with the L858R and del19 activating EGFR mutations are responsive to the quinazolines gefitinib and erlotinib. However, resistance to these agents typically emerges after a year, primarily

[1]Current Address: Department of Chemistry, University of Buffalo, Buffalo, NY 14260, USA

[2]Current Address: Department of Medicinal Chemistry and Department of Chemistry and Systems Biology, Stanford University, Stanford, CA 94305, USA.

Supplementary data

Supplementary data to this article can be found online at:

Declaration of interests

The authors declare that they have no known competing financial interests or personal relationships that could have appeared to influence the work reported in this paper.

through the T790M gatekeeper mutation, which enhances affinity for ATP and renders the inhibitors less able to compete.[4] Second-generation EGFR inhibitors such as afatinib and dacomitinib attempted to address this through covalent bond formation with a cysteine adjacent to the ATP site, but activity against wild-type (wt) EGFR led to gastrointestinal toxicity and a limited therapeutic index for these agents in the clinic.

The third-generation covalent inhibitor osimertinib was developed from a series of pyrimidines with selectivity for oncogenic EGFR mutants over wild-type (wt) EGFR.[5, 6] The combination of efficacy and improved tolerability led to initial FDA approval in 2015 for T790M-positive patients, and the drug progressed to first line therapy for metastatic NSCLC in 2018. As with other kinase inhibitors, however, resistance emerges, and in common with other covalent inhibitors, this often involves the cysteine residue critical to the molecule's activity. In patients treated with both osimertinib and a first-generation inhibitor, C797S is the most frequently observed mutation, and there are currently no targeted therapies for patients who have progressed to $EGFR^{L858R/T790M/C797S}$ status. Other mechanisms of resistance to osimertinib include the activation of the MEK signaling pathway, and amplification of wt EGFR.[7] Most kinase inhibitors target the ATP site, and while there are some highly selective compounds, achieving selectivity across the kinome can be a challenge. Activity against two or more kinases may be beneficial in some cases, but non-selective inhibitors may have limited tolerability and be unsuitable for combination with other therapies. Allosteric inhibitors which bind outside the ATP pocket can be exquisitely selective, have greater potential for use in combination with other therapies,[8] and may delay the onset of resistance in earlier lines of therapy when combined with existing agents.

EAI045 (Fig. 1) was identified as an allosteric EGFR inhibitor following a HTS campaign to find non-ATP competitive compounds with selectivity for the $EGFR^{L858R/T790M}$ mutant over wt EGFR.[9] It binds to the inactive conformation of EGFR in a pocket adjacent to the ATP site. Upon activation through ligand binding, EGFR forms asymmetrical dimers in which the allosteric site is less accessible in the activator subunit. This blocks the binding of EAI045, and as a single agent it has minimal cellular and *in vivo* activity. The addition of cetuximab prevents dimer formation, and the combination with EAI045 demonstrated good activity in $EGFR^{L858R/T790M}$ models. Optimization of the isoindolinone series identified JBJ-04-125-02 (Fig. 1), with a phenyl piperazine substituent extending into a channel alongside the α-helix. The enhanced potency of JBJ-04-125-02 enables it to achieve good single-agent activity in a Ba/F3 $EGFR^{L858R/T790M}$ cell antiproliferative assay.[10] In mice, the compound has low *in vivo* clearance and a high volume of distribution, but poor oral bioavailability (Table 1). Despite its disappointing oral PK profile, efficacy was observed in an H1975 model upon daily oral dosing at 100 mg/kg. Additionally, the allosteric inhibitors co-bind with osimertinib,[11] and the combination with JBJ-04-125-02 delivered enhanced effects relative to the individual agents in a set of *in vitro* and *in vivo* studies.[10]

We attempted to improve permeability and bioavailability by reducing the number of H-bond donors in the molecule, and prepared *N*-methyl piperazine **3** and *N*-methyl piperidine JBJ-09-063. These changes did not significantly impact oral exposure, but the enhanced potency of JBJ-09-063 supported its use as an improved *in vivo* tool compound

(Table 1), and JBJ-09-063 achieved tumor regression in osimertinib-resistant triple mutant ($EGFR^{L858R/T790M/C797S}$) models upon daily oral dosing at 50 mg/kg.[12] At the same dose, minimal effects were observed with JBJ-09-063 in an A431 (wt EGFR) efficacy model. The removal of the phenol to give compound **5** led to a reduction in potency, without any improvement in oral bioavailability (Table 1).

Our screening cascade consisted of an $EGFR^{L858R/T790M}$ enzyme assay,[13] and a Ba/F3 cellular proliferation assay with two readouts, one measuring compound activity as a single agent, and one with the addition of cetuximab to prevent the formation of EGFR dimers.[13] Few of the early project compounds showed good cellular potency as single agents, and the second readout generated useful cell SAR for less potent examples. The objective was an agent for the treatment of osimertinib-resistant NSCLC, but we observed an excellent correlation between the $EGFR^{L858R/T790M}$ and $EGFR^{L858R/T790M/C797S}$ mutants in both enzyme and Ba/F3 cell assays, and we retained the $EGFR^{L858R/T790M}$ assays as our primary screens to provide consistency with historic project data. Ba/F3 $EGFR^{L858R/T790M/C797S}$ cell data was collected later for selected compounds, with this assay showing increased sensitivity to the allosteric inhibitors. Enzyme IC_{50} data correlated with the cellular data for cetuximab co-treatment but less so for compounds dosed as a single agent. We attributed this to asymmetric EGFR dimer formation in the cell, where one allosteric site is less accessible, and we observed an enzyme IC_{50} threshold of about 1 nM to achieve single-agent cell potency of <1 μM in the $EGFR^{L858R/T790M}$ assay.

JBJ-09-063 was sufficiently stable to deliver good efficacy upon oral dosing, but under certain conditions it underwent hydrolysis to the corresponding acid, presumably via intramolecular lactone formation. To develop allosteric EGFR inhibitors for osimertinib-resistant NSCLC, we wanted to avoid the potential chemical instability present in compounds that incorporated both the thiazole amide and phenol groups. The SAR around the thiazole was very tight, with little tolerance for even small substituents or replacements other than 2-pyridine. Another group reported an attempt to mitigate the hydrolysis risk by replacing the thiazole amide of EAI045 with a bicyclic quinazolinone group, but this led to a dramatic reduction in potency.[14] A patent application from the same group disclosed a series of isoindolinones in which the thiazole amide was replaced by indoles and benzimidazoles, with more promising activity data.[15]

At the phenyl position, the 5-fluoro-2-phenol is preferred, but moderate potency is retained with an unsubstituted phenyl (**6-7**) or 3-fluorophenyl ring (**5, 8**, Table 2). As part of our efforts to develop chemically stable EGFR inhibitors, we removed the phenol moiety, and sought to improve the overall potency and PK profile through modifications elsewhere. Extensive exploration of the right-hand side of the isoindolinone series had culminated in the exquisite potency of JBJ-09-063, and we instead focused on replacements of the isoindolinone core. We acknowledged that new scaffolds might require re-optimization of the right-hand side, but initially incorporated *N*-methyl piperazine and *N*-methyl piperidine to deliver matched pairs with the isoindolinone series. We introduced the aryl amine at both the 6 and 7 positions of the dihydroisoquinolinone to determine if there was any preference for the positioning of this substituent in the channel revealed by our previous structural work.

We first expanded the lactam ring of the isoindolinone to generate dihydroisoquinolinones, incorporating the 3-F-phenyl substituent to give compounds **9-12** as the matched pairs of isoindolinones **5** and **8** (Table 2). Compounds were prepared according to Scheme 1. The lactones **13** were treated with $POCl_3$ to give the corresponding chloroethyl acid chlorides, to which the 3-F phenylglycine ester was added to form the amides. The amides were cyclized to the bicyclic lactams **14** by treatment with potassium *t*-butoxide in refluxing dioxane. Ester hydrolysis and coupling of the acid with 2-aminothiazole gave the amides **15**, with Suzuki couplings with the phenylpiperazine or phenylpiperidine boronate to generate the final compounds **9-12**. Disappointingly, these compounds showed reduced enzyme and cellular potency relative to the corresponding isoindolinones regardless of the regiochemistry of the substituent (e.g. **10** or **12** v **5**). Consistent with the isoindolinone pair **3** and JBJ-09-063, the piperidine example was usually more potent than the corresponding piperazine in both the enzyme and cellular assays.

We next prepared examples **16-27** in the isoquinolinone, quinazolinone and phthalazinone series (Table 3). Alkylation of the bicyclic cores **28** with methyl 2-bromo-2-phenylacetate gave the bromoesters **29**, followed by chemistry similar to that described for the dihydroisoquinolinone scaffold (Scheme 2).[13] As before, examples with a piperidine were more potent than the corresponding piperazines. For the isoquinolinone scaffold, we observed a slight preference for 6-substituents across the set of matched pairs (**16** v **18** and **17** v **19**). For the quinazolinones, substituents at the 6-position were clearly favored (**22** v **20**, **23** v **21**). In the numbering system for these bicyclic series, the 6-position is on the same side of the core as the carbonyl for the quinazolinones, but the opposite side for the isoquinolinones and phthalazinones. Compound **23** was the most potent quinazolinone, with an IC_{50} of 0.2 nM, and a cell EC_{50} of 0.72 μM and 0.05 μM as a single agent in our Ba/F3 $EGFR^{L858R/T790M}$ and $EGFR^{L858R/T790M/C797S}$ assays respectively. The phthalazinones **24-27** were less potent across both the enzyme and cell assays.

Examples from both the isoquinolinone and quinazolinone series showed promising activity, comparable and in some cases better than their isoindolinone matched pairs (**6, 7**, Table 2). We were conscious of the high lipophilicity of the series and prepared examples with an additional nitrogen in the core (**31-32**, Table 4). Inspired by the dramatic potency enhancement achieved with a fluorine scanning approach on a similar scaffold in a series of Bruton's tyrosine kinase (BTK) inhibitors,[16] we also introduced fluorine at different positions of the quinazolinone (**33-35**). We prioritized compounds with the phenyl piperidine substituent at the 6-position of these scaffolds, as this regiochemistry had been preferred in the initial quinazolinone examples.

These series could not be readily accessed by the synthetic route of Scheme 2, as the additional nitrogen atom or fluorine substituent appeared to render the alkylated cores unstable to the basic conditions used in the ester hydrolysis step. Azaquinazolinones **31** and **32** were instead prepared from 6-bromopyrido[3,2-d]pyrimidin-4(3H)-one and 6-bromopyrido[2,3-d]pyrimidin-4(3H)-one respectively by alkylation with methyl 2-bromo-2-phenylacetate to give the esters **37** (Scheme 3). This was followed by Suzuki couplings to install the phenyl piperidine. This reaction could be stopped to give the corresponding

esters, but prolonged heating resulted in hydrolysis to the acids **38**, which were coupled with 2-aminothiazole to generate the target compounds **31** and **32**.

8-F-Quinazolinone **33** was prepared by similar chemistry, from the commercially available starting material 6-bromo-8-fluoroquinazolin-4(3H)-one (**36**, X=CH, Y = CF). For **34**, the nitrile of 6-amino-3-bromo-2-fluorobenzonitrile **39** was hydrolyzed to the acid, followed by an amide coupling with methyl 2-amino-2-phenylacetate to give **40**. Cyclization to the 5-F quinazolinone was achieved by heating **40** in neat triethylorthoformate, with the usual Suzuki and amide couplings to complete the synthesis.

The 7-F quinazolinone **35** was synthesized by a different route (Scheme 3). Amino amide **42** was prepared from Boc-protected 2-aminophenylacetic acid **41**. A Suzuki coupling installed the phenyl piperidine onto 6-bromo-7-fluoroquinazolin-4(3H)-one **43** to give **44**, and this was coupled with amine **42** via HATU activation[17] to give **35**.

The 5-F quinazolinone **34** was the most potent of this set of compounds and showed a significant improvement in potency relative to the corresponding isoindolinone **7**, with an $EGFR^{L858R/T790M}$ IC_{50} of 0.1 nM, and cell EC_{50}s of 0.32 μM and 0.02 μM in our Ba/F3 $EGFR^{L858R/T790M}$ and $EGFR^{L858R/T790M/C797S}$ assays respectively (Table 4).

We obtained a co-crystal structure of **34** binding to $EGFR^{T790M/V948R}$. The V948 residue is distant from the binding site and was introduced to prevent EGFR asymmetric dimer formation during crystallization. The structure confirmed that the quinazolinone series binds in essentially the same manner as the isoindolinones,[10, 12] though lacking the hydrogen bond of the phenolic OH to the backbone of F856. The amide NH forms a key H-bond interaction with D855, and the quinazolinone core positions the phenyl piperidine substituent into the groove adjacent to the α-C-helix to enable the piperidine nitrogen to interact with acidic residue E758.

We obtained *in vivo* rat PK (1 mg/kg IV, 10 mg/kg PO) for 5-F-quinazolinone **34**. It was found to have moderate IV Cl (30 mL/min/kg), $T_{1/2}$ of 3.5 hours and oral bioavailability of 24%. Compound **34** was profiled in an H1975 tumor efficacy model ($EGFR^{L858R/T790M}$) and achieved tumor regression upon oral dosing at both the 25 mg/kg and 50 mg/kg doses administered once daily, with slower re-growth post-treatment at the higher dose. The compound was well-tolerated at both doses.

In conclusion, we pursued a scaffold-hopping approach to identify new series of allosteric mutant-selective EGFR inhibitors, with good activity against the $EGFR^{L858R/T790M}$ and $EGFR^{L858R/T790M/C797S}$ mutants. The 5-fluoroquinazolinone scaffold delivered a compound with sufficient potency to achieve good *in vivo* efficacy without the need for the fluorophenol group, mitigating the potential chemical instability risk. Our further efforts to develop an agent for the treatment of osimertinib-resistant NSCLC will be reported in due course.

Supplementary Material

Refer to Web version on PubMed Central for supplementary material.

Acknowledgments

We thank Takeda Pharmaceuticals for funding support and scientific discussions. The rat PK study was conducted at WuXi AppTec. T.S.B is supported by a Ruth L. Kirschstein National Research Service Award (1F32CA247198-01). The crystallography work is based upon research conducted at the Northeastern Collaborative Access Team beamlines (P30 GM124165, P41 GM103403) utilizing resources of the Advanced Photon Source at the Argonne National Laboratory (DE-AC02-06CH11357).

References and notes

1. Roskoski R Jr. Properties of FDA-approved small molecule protein kinase inhibitors: A 2021 update. Pharmacol Res. 2021;165:105463. doi: 10.1016/j.phrs.2021.105463. [PubMed: 33513356]
2. Xie Z, Yang X, Duan Y, Han J, Liao C. Small-Molecule Kinase Inhibitors for the Treatment of Nononcologic Diseases. J Med Chem. 2021;64(3):1283–345. doi: 10.1021/acs.jmedchem.0c01511. [PubMed: 33481605]
3. Ayati A, Moghimi S, Salarinejad S, Safavi M, Pouramiri B, Foroumadi A. A review on progression of epidermal growth factor receptor (EGFR) inhibitors as an efficient approach in cancer targeted therapy. Bioorg Chem. 2020;99:103811. doi: 10.1016/j.bioorg.2020.103811. [PubMed: 32278207]
4. Yun CH, Mengwasser KE, Toms AV, Woo MS, Greulich H, Wong KK, et al. The T790M mutation in EGFR kinase causes drug resistance by increasing the affinity for ATP. Proc Natl Acad Sci U S A. 2008;105(6):2070–5. doi: 10.1073/pnas.0709662105. [PubMed: 18227510]
5. Ward RA, Anderton MJ, Ashton S, Bethel PA, Box M, Butterworth S, et al. Structure- and reactivity-based development of covalent inhibitors of the activating and gatekeeper mutant forms of the epidermal growth factor receptor (EGFR). J Med Chem. 2013;56(17):7025–48. doi: 10.1021/jm400822z. [PubMed: 23930994]
6. Finlay MR, Anderton M, Ashton S, Ballard P, Bethel PA, Box MR, et al. Discovery of a potent and selective EGFR inhibitor (AZD9291) of both sensitizing and T790M resistance mutations that spares the wild type form of the receptor. J Med Chem. 2014;57(20):8249–67. doi: 10.1021/jm500973a. [PubMed: 25271963]
7. Schmid S, Li JJN, Leighl NB. Mechanisms of osimertinib resistance and emerging treatment options. Lung Cancer. 2020;147:123–9. doi: 10.1016/j.lungcan.2020.07.014. [PubMed: 32693293]
8. Lu X, Smaill JB, Ding K. New Promise and Opportunities for Allosteric Kinase Inhibitors. Angew Chem Int Ed Engl. 2020;59(33):13764–76. doi: 10.1002/anie.201914525. [PubMed: 31889388]
9. Jia Y, Yun CH, Park E, Ercan D, Manuia M, Juarez J, et al. Overcoming EGFR(T790M) and EGFR(C797S) resistance with mutant-selective allosteric inhibitors. Nature. 2016;534(7605):129–32. doi: 10.1038/nature17960. [PubMed: 27251290]
10. To C, Jang J, Chen T, Park E, Mushajiang M, De Clercq DJH, et al. Single and Dual Targeting of Mutant EGFR with an Allosteric Inhibitor. Cancer Discov. 2019;9(7):926–43. doi: 10.1158/2159-8290.CD-18-0903. [PubMed: 31092401]
11. Niggenaber J, Heyden L, Grabe T, Muller MP, Lategahn J, Rauh D. Complex Crystal Structures of EGFR with Third-Generation Kinase Inhibitors and Simultaneously Bound Allosteric Ligands. ACS Med Chem Lett. 2020;11(12):2484–90. doi: 10.1021/acsmedchemlett.0c00472. [PubMed: 33335671]
12. To C, et al. , Molecular basis for cooperative binding and synergy of ATP-site and allosteric EGFR inhibitors. Nature Cancer. 2022, accepted for publication.
13. Gray NS, Scott DA, Gero T, Eck M, Heppner D, Beyett T, et al. Nitrogen containing heterocycles as allosteric EGFR inhibitors and preparation and methods of use thereof. PCT Int. Appl. WO2020257632.
14. Lee S, Kim J, Duggirala KB, Go A, Shin I, Cho BC, et al. Allosteric Inhibitor TREA-0236 Containing Non-hydrolysable Quinazoline-4-one for EGFR T790M/C797S Mutants Inhibition. Bulletin of the Korean Chemical Society. 2018;39(7):895–8. doi: 10.1002/bkcs.11491.
15. Lee K, Choi G, Lee S, Kim J, Cho B, Park CW, Yun J. Isoindolin-1-one derivative, method for preparing same, and pharmaceutical composition comprising same as effective component for preventing or treating cancer. PCT Int. Appl WO2020036386.

16. Lou Y, Sweeney ZK, Kuglstatter A, Davis D, Goldstein DM, Han X, et al. Finding the perfect spot for fluorine: improving potency up to 40-fold during a rational fluorine scan of a Bruton's Tyrosine Kinase (BTK) inhibitor scaffold. Bioorg Med Chem Lett. 2015;25(2):367–71. doi: 10.1016/j.bmcl.2014.11.030. [PubMed: 25466710]

17. Xiao Z, Yang MG, Li P, Carter PH. Synthesis of 3-substituted-4(3H)-quinazolinones via HATU-mediated coupling of 4-hydroxyquinazolines with amines. Org Lett. 2009; 11(6):1421–4. doi: 10.1021/o1802946p. [PubMed: 19243133]

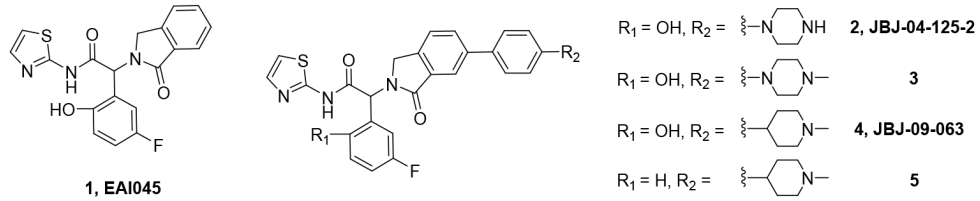

Fig. 1 –.
structures of EAI045 and optimized isoindolinones

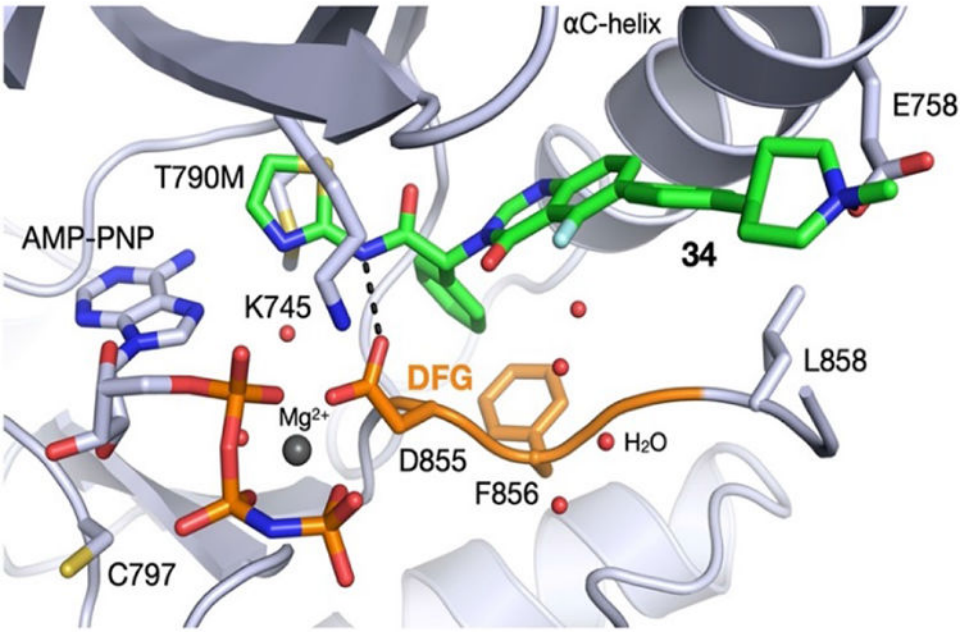

Fig. 2 –.

Co-crystal structure of $EGFR^{T790M/V948R}$ bound to **34** and AMP-PNP (2.3 Å, PDB 7LTX)

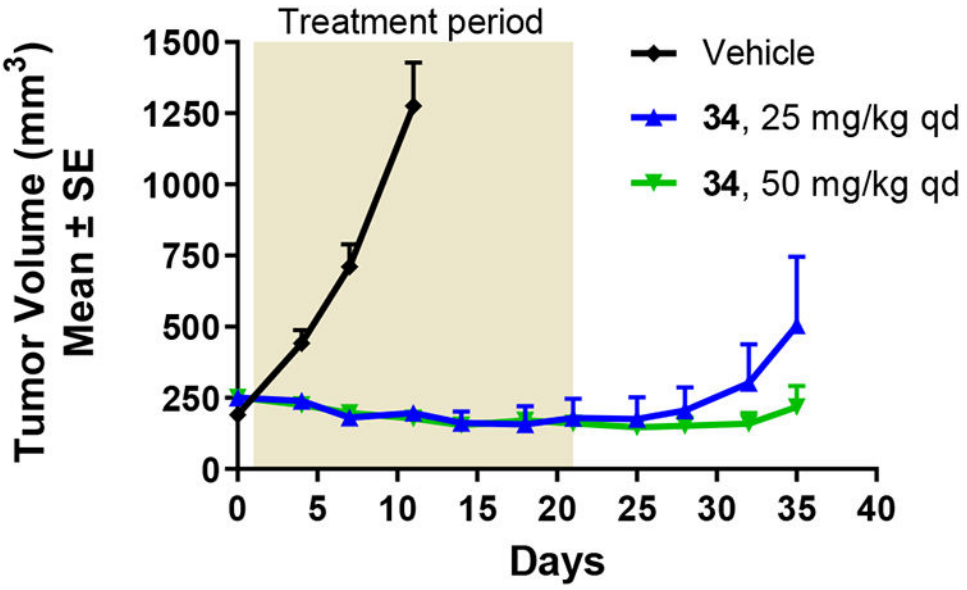

Fig. 3 –.
H1975 efficacy data for compound **34**.

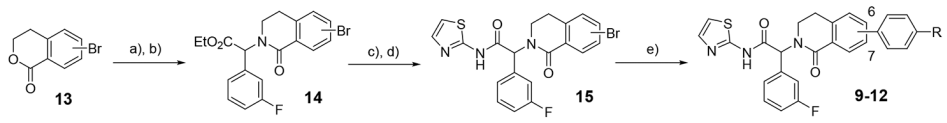

Scheme 1 –.

synthesis of dihydroisoquinolinones **9-12.** Reagents and conditions: a) PCl_5, $POCl_3$, reflux; b) ethyl 2-amino-2-(3-fluorophenyl)acetate, $^{i}Pr_2NEt$, THF, 0°C, then $KO^{t}Bu$, dioxane, 110°C, 23-35% over two steps; c) $LiOH.H_2O$, THF, MeOH, 76-97%; d) 2-aminothiazole, $^{i}Pr_2NEt$, HATU, DMF, 55°C, 38-73%; e) aryl amine pinacol boronate, $Pd(dppf)Cl_2$, Na_2CO_3, 4:1 dioxane:water, 105°C, 49-59%.

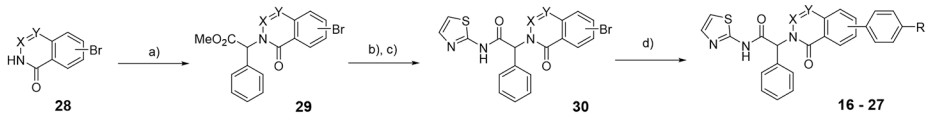

Scheme 2 –.

synthesis of compounds **16-27.** Reagents and conditions: a) methyl 2-bromo-2-phenylacetate, Cs_2CO_3, DMF, 50°C, 55-79%; b) LiOH, H_2O, MeOH, THF, 27-99%; c) 2-aminothiazole, $^{i}Pr_2NEt$, HATU, DMF, 60°C, 56-85%; d) aryl amine pinacol boronate, $Pd(dppf)Cl_2$, Na_2CO_3, 4:1 dioxane:water, 100°C, 24-70%.

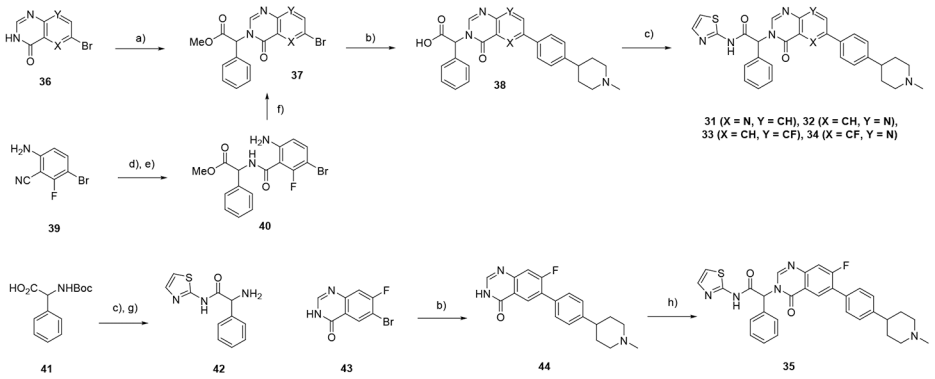

Scheme 3 –.

synthesis of compounds **31-35.** Reagents and conditions: a) methyl 2-bromo-2-phenylacetate, Cs_2CO_3, DMF, 50°C, 24-60%; b) 1-methyl-4-(4-(4,4,5,5-tetramethyl-1,3,2-dioxaborolan-2-yl)phenyl) piperidine, $Pd(dppf)Cl_2$. Na_2CO_3, 4:1 dioxan:water, 100°C, 11-59%; c) 2-aminothiazole, $^{i}Pr_2NEt$, HATU, DMF, 60°C, 9-48%; d) LiOH, water, 100°C, 88%; e) methyl 2-amino-2-phenylacetate, $^{i}Pr_2NEt$, HATU, DMF, 72%; f) $(EtO)_3CH$, reflux, 79%; g) TFA, DCM; h) **42**, HATU, DBU, CH_3CN, 7%.

Table 1

EGFR$^{L858R/T790M}$ enzyme and Ba/F3 cell data, and mouse *in vivo* PK (3 mg/kg IV, 20 mg/kg PO) for isoindolinones

Cpd	Enzyme IC_{50} (nM)	Cell IC_{50} (μM)	Cell IC_{50} (μM)+cetux	IV Cl (mL/min/kg)	IV $T_{1/2}$ (hr)	Vss (L/kg)	F %	Auc 8hr (ng*hr/mL)
1, EAI045	3.3	> 10.0	0.221	-	-	-	-	-
2, JBJ-04-125-02	0.3	0.61	0.021	5.0	3.0	0.6	3	2523
3	0.3	0.49	0.006	10.3	2.8	1.8	2	1351
4, JBJ-09-063	0.1	0.05	0.006	15.7	2.3	2.5	15	2398
5	0.2	1.07	0.020	13.9	3.1	2.4	4	1002

Table 2

EGFR$^{L858R/T790M}$ enzyme and Ba/F3 cell activity of isoindolinones (A) and dihydroisoquinolinones (B)

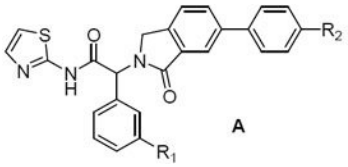

A

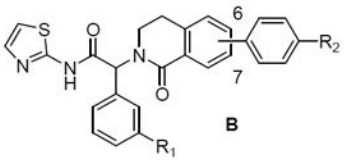

B

Cpd	Core	R_1	R_2	Enzyme IC_{50} (nM)	L858R/T790M Cell IC_{50} (μM)	L858R/T790M Cetux co-dosing Cell IC_{50} (μM)	L858R/T790M /C797S Cell IC_{50} (μM)
6	A	H	*N*-Me piperazine	0.9	2.56	0.043	-
7	A	H	*N*-Me piperidine	0.9	1.00	0.020	0.179
8	A	F	*N*-Me piperazine	1.8	1.99	0.044	-
5	A	F	*N*-Me piperidine	0.2	1.07	0.020	0.152
9	B	F	6, *N*-Me piperazine	1.1	3.66	0.801	-
10	B	F	6, *N*-Me piperidine	2.2	1.99	0.246	-
11	B	F	7, *N*-Me piperazine	6.8	1.60	0.126	-
12	B	F	7, *N*-Me piperidine	3.2	1.47	0.099	-

Table 3

EGFR$^{L858R/T790M}$ enzyme and Ba/F3 cell activity of isoquinolinones (C), quinazolinones (D) and phthalazinones (E) **16-27**

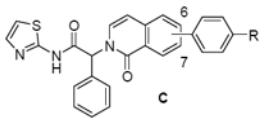

C

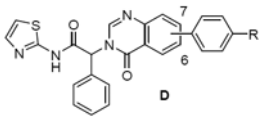

D

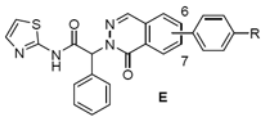

E

Cpd	Core	R	Enzyme IC_{50} (nM)	L858R/T790M Cell IC_{50} (μM)	L858R/T790M Cetux co-dosing Cell IC_{50} (μM)	L858R/T790M /C797S Cell IC_{50} (μM)
7			0.9	1.00	0.020	0.18
16	C	6, *N*-Me piperazine	3.4	1.27	0.062	-
17	C	6, *N*-Me piperidine	1.2	1.28	0.024	0.50
18	C	7, *N*-Me piperazine	5.0	1.85	0.044	-
19	C	7, *N*-Me piperidine	1.8	1.50	0.070	0.38
20	D	7, *N*-Me piperidine	3.1	2.00	0.375	-
21	D	7, *N*-Me piperidine	5.8	2.43	0.225	0.90
22	D	6, *N*-Me piperidine	0.9	2.32	0.021	-
23	D	6, *N*-Me piperidine	0.2	0.78	0.007	0.05
24	E	6, *N*-Me piperidine	17.8	3.46	1.67	-
25	E	6, *N*-Me piperidine	9.7	1.24	0.538	0.99
26	E	7, *N*-Me piperidine	10.3	2.16	0.380	-
27	E	7, *N*-Me piperidine	4.0	1.54	0.207	0.44

Table 4

EGFR$^{L858R/T790M}$ enzyme and cell potency of azaquinazolinones **31-32** and F-quinazolinones **33-35**

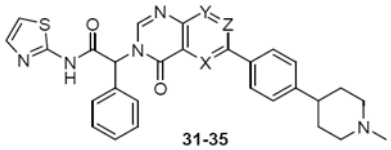

31-35

Cpd	X	Y	Z	Enzyme IC_{50} (nM)	L858R/T790M Cell IC_{50} (μM)	L858R/T790M Cetux co-dosing Cell IC_{50} (μM)	L858R/T790M /C797S Cell IC_{50} (μM)
7				0.9	1.00	0.020	0.18
31	N	CH	CH	0.6	1.71	0.016	0.09
32	CH	N	CH	1.9	1.14	0.023	0.31
33	CH	CF	CH	0.6	0.81	0.010	0.15
34	CF	CH	CH	0.1	0.32	0.003	0.02
35	CH	CH	CF	1.4	3.00	0.073	0.28